# Museomics reduces taxonomic inflation in the Dendropsophus araguaya complex (Hylinae: Dendropsophini) from the Cerrado

Authors: Nakamura, Daniel Y.M., Orrico, Victor G.D., Da Silva, Esdras M.G., Lyra, Mariana L., and Grant, Taran

Source: Journal of Vertebrate Biology, 74(24112)

Published By: Institute of Vertebrate Biology, Czech Academy of Sciences

URL: https://doi.org/10.25225/jvb.24112

Journal of Vertebrate Biology

Open Access

J. Vertebr. Biol. 2025, 74: 24112 DOI: 10.25225/jvb.24112

RESEARCH PAPER

# Museomics reduces taxonomic inflation in the *Dendropsophus araguaya* complex (Hylinae: Dendropsophini) from the Cerrado

Daniel Y.M. NAKAMURA[1,2], Victor G.D. ORRICO[3], Esdras M.G. DA SILVA[1], Mariana L. LYRA[4] and Taran GRANT[1*]

[1] *Laboratório de Anfíbios, Departamento de Zoologia, Instituto de Biociências, Universidade de São Paulo, Rua do Matão, Cidade Universitária, São Paulo, Brazil; e-mail: dani_ymn@usp.br, matheusdras@gmail.com, taran.grant@ib.usp.br*

[2] *Division of Invertebrate Zoology, American Museum of Natural History, New York, USA*

[3] *Laboratório de Herpetologia Tropical, Departamento de Ciências Biológicas, Universidade Estadual de Santa Cruz, Rodovia Jorge Amado, Ilhéus, Bahia, Brazil; e-mail: vgdorrico@uesc.br*

[4] *New York University Abu Dhabi, Saadiyat Island, Abu Dhabi, United Arab Emirates; e-mail: marillyra@gmail.com*

Received 9 October 2024; Accepted 11 December 2024; Published online 6 February 2025

**Abstract.** The systematics of the *Dendropsophus araguaya* complex requires a reassessment due to the unknown position of *D. rhea*, possible misidentifications of *D. tritaeniatus*, the polyphyly of *D. araguaya* and *D. jimi* recovered in a recent total evidence analysis, and intraspecifically variable characters used in diagnoses. We successfully assembled historical DNA from formalin-fixed paratopotype specimens of *D. rhea* and *D. tritaeniatus* collected in 1952 and 1963, respectively. Our results revealed that *D. rhea* is nested within a clade formed by *D. cerradensis* and *D. jimi*. Combining evidence from phylogeny, genetic distances, and morphology, we propose that *D. jimi* and *D. rhea* are junior synonyms of *D. cerradensis*. We corroborate the polyphyly of topotypic *D. araguaya*, with one clade nested within *D. cerradensis sensu novo* and another that includes a paratopotype of *D. tritaeniatus*; however, hDNA of the holotype of *D. araguaya* was not successfully assembled, so we consider *D. araguaya* to be *incertae sedis*. We update the name of the *D. araguaya* complex to the *D. cerradensis* complex. Furthermore, we also reveal that some specimens previously identified as *D. tritaeniatus* are *D. cachimbo*. Our study illustrates the ability of museomics to clarify the taxonomic identity and phylogenetic relationships of possibly extinct species and reduce taxonomic inflation in amphibian systematics.

**Key words:** Anura, archival DNA, extinct species, historical DNA, successive outgroup sampling expansion, synonyms

## Introduction

Museomics aims to obtain highly degraded historical DNA sequences (hDNA) from natural history collections (Raxworthy & Smith 2021) and is especially relevant for conservation and systematics. In conservation, hDNA allows researchers to document the genetic diversity of extinct species, clarify past disease dynamics, provide a potential baseline for de-extinction (Shapiro 2017, Blair 2024),

* *Corresponding Author*

and update the conservation status of lost species (i.e. disappeared for decades in nature but not formally declared to be extinct; Martin et al. 2022) in light of a revised taxonomy. In systematics, museomics enables phylogenetic relationships to be tested (e.g. Lyra et al. 2020, Ernst et al. 2021) and the taxonomic identity of lost species for which modern tissues are unavailable to be elucidated. For instance, recent studies employed hDNA to describe cryptic species (e.g. Rancilhac et al. 2020, Mahony et al. 2022) or synonymise conspecifics (e.g. Reyes-Velasco et al. 2021). As such, museomics is fundamental to address both the Darwinian (i.e. evolutionary problems such as the position of lost species; Diniz-Filho et al. 2013) and Linnean shortfalls (i.e. taxonomic problems such as the status of species with poorly defined diagnostic characters; Whittaker et al. 2005).

Darwinian and Linnean shortfalls are prevalent in *Dendropsophus* Fitzinger, 1843, a hylid genus comprising 107 species of small tree frogs primarily distributed in South America (Frost 2024). Faivovich et al. (2005) resurrected *Dendropsophus* for the species of *Hyla* Laurenti, 1768, known or suspected to have 30 chromosomes (Duellman & Cole 1965, Duellman & Crump 1974, Duellman & Trueb 1983). Recently, Orrico et al. (2021) conducted a total evidence analysis of Dendropsophini, recognising nine species groups of *Dendropsophus*. Specifically, five clades were recognised within the *D. microcephalus* group, including the *D. bipunctatus*, *D. branneri*, *D. microcephalus*, *D. nanus*, and *D. rubicundulus* clades.

The *D. rubicundulus* clade comprises 11 species distributed throughout the Brazilian Cerrado and adjacent regions of Argentina, Bolivia, and Paraguay (Frost 2024). They are characterised by their green dorsum in life (violet in preservative), except *D. sanborni* (Schmidt, 1944) and *D. rozenmani* Jansen et al. 2019, which have pale pinkish hues dorsally (Orrico et al. 2021). Napoli & Caramaschi (1998, 1999a, b, 2000) recognised two species complexes based on the number of sacral stripes: the *D. tritaeniatus* complex for species with a single sacral stripe and the *D. rubicundulus* complex for those with double sacral stripes. Orrico et al. (2021) refuted the monophyly of those species complexes, recognising instead 1) the *D. anataliasiasi* complex for *D. anataliasiasi* (Bokermann, 1972), *D. elianae* (Napoli & Caramaschi, 2000), *D. sanborni*, and *D. rubicundulus* (Reinhardt & Lütken, 1862), and 2) the *D. araguaya* complex for *D. araguaya* (Napoli & Caramaschi, 1998), *D. cachimbo* (Napoli & Caramaschi, 1999a), *D. cerradensis* (Napoli & Caramaschi, 1998), *D. jimi* (Napoli & Caramaschi, 1999b), *D. rozenmani*, and *D. tritaeniatus* (Bokermann, 1965).

The *D. araguaya* complex comprises green treefrogs (except the brown *D. rozenmani*) distributed in Bolivia, Brazil, and Paraguay (Frost 2024) with three dorsal stripes (except *D. cachimbo*; see Table 2 in Napoli & Caramaschi 1999b). At least four problems in the systematics of the *D. araguaya* complex remain unresolved. First, *D. rhea* (Napoli & Caramaschi, 1999b) is only known from the type locality (Cachoeira das Emas, Pirassununga, São Paulo, Brazil) and has not been observed since 1963, and its phylogenetic position is unknown (Orrico et al. 2021). Second, although *D. tritaeniatus* has been reported in streams ca. 70 km from the type locality (São Vicente, Mato Grosso, Brazil; e.g. Teixeira et al. 2013), topotypic DNA sequences are unavailable, which could resolve potential misidentifications of *D. tritaeniatus* from the literature. For instance, without explanation, Arantes et al. (2023) and Portik et al. (2023) re-identified some sequences of *D. cachimbo* and *D. rozenmani* from GenBank as *D. tritaeniatus.* Third, in their total evidence analysis, Orrico et al. (2021) recovered *D. araguaya* and *D. jimi* as polyphyletic. In the case of *D. araguaya*, the two analysed topotypic samples were recovered as independent lineages referred to as *D. araguaya* I and *D. araguaya* II. Fourth, most diagnostic characters in the *D. araguaya* complex are intraspecifically variable and thus not diagnostic (e.g. protuberance of eyes and orientation of dorsal stripes; V.G.D. Orrico, pers. observ.).

Here we aim to 1) test the phylogenetic relationships of *D. rhea* using hDNA sequences from a paratopotype, 2) re-evaluate potential misidentifications of *D. tritaeniatus* in previous studies based on morphological study and hDNA sequences from a paratopotype of *D. tritaeniatus*, and 3) assess the taxonomic identity of *D. araguaya* using hDNA from the holotype, modern DNA from topotypic samples, and morphology. We also propose taxonomic changes on the basis of our results and discuss the validity of previously reported diagnostic characters employed in the *D. araguaya* complex.

## Material and Methods

### Historical DNA

Fresh tissues for DNA sequencing are unavailable for *D. rhea*. Fresh tissues identified as *D. araguaya* and *D. tritaeniatus* are available, but their taxonomic identity is problematic (e.g. Orrico et al. 2021, Arantes et al. 2023, Portik et al. 2023), requiring data from

paratopotype or holotype samples for clarification. Following Nakamura et al. (2024), we sampled ca. 0.5 $mm^3$ of muscle from an unexposed region of the trunk via a short dorsolateral incision on formalin-fixed paratopotypes of *D. rhea* (MZUSP 14458, collected 3 November 1952 by Pietracatelli, Seraglia, and W.C.A. Bokermann in Cachoeira de Emas, Pirassununga, São Paulo, Brazil) and *D. tritaeniatus* (MZUSP 73973, collected 28 November 1963 by M. Alvarenga, F.M. Oliveira, and W.C.A. Bokermann in São Vicente, Mato Grosso, Brazil), as well as the holotype of *D. araguaya* (MZUSP 66803, collected 20 March 1989 by J.P. Caldwell in Alto Araguaia, Mato Grosso, Brazil; Appendix S1).

We followed recommended procedures to avoid cross-contamination (Llamas et al. 2017, Fulton & Shapiro 2019, Straube et al. 2021), and all procedures before PCR amplification were performed in a dedicated cleanroom laboratory in the Department of Zoology, Institute of Biosciences, University of São Paulo. We washed tissues with 1 mL phosphate buffer saline solution to decrease the amount of potential inhibitors (e.g. formaldehyde). We extracted DNA using the proteinase K treatment (Straube et al. 2021) and DNA purification following Dabney et al. (2013). We prepared dual-indexed single-stranded DNA libraries, with excision of uracil and abasic sites carried out by uracil-DNA glycosylase and endonuclease VIII, respectively (Gansauge et al. 2017). Finally, we performed high-throughput DNA sequencing in Illumina Nextseq 500/550 platform (500/550 High Output v2.5; 75 cycles; single-end reads) at TUCF Genomics (Tufts University School of Medicine, Boston, MA).

Bioinformatic analyses comprised three steps: data preprocessing, read mapping, and consensus calling. First, we assessed read quality using FASTQC v. 0.12.1 (Andrew 2010), trimmed Illumina adapters and < 21 bp reads using Cutadapt v. 1.16 (Martin 2011) and removed PCR duplicates using Tally (Davis et al. 2013), filtered out contaminant reads from human and bacterial references (e.g. *Escherichia coli* and *Paraburkholderia* sp.) using FastqScreen v. 0.15.3 (Wingett & Andrews 2018), and summarised results from data preprocessing using FastQC (Andrew 2010). Second, we performed baiting and iterative read mapping using the MIRA v. 4.0.2 assembler in MITObim v. 1.8 script (Hahn et al. 2013), choosing parameters (mismatch = 3 and k-bait = 15) and initial reference seeds (*D. microcephalus*; GenBank accession numbers: MT503852 (H-strand transcription unit 1, H1, composed of 12S rRNA, $tRNA^{Val}$, and 16S rRNA), MT483137 (cytochrome *c* oxidase I, *COI*), MT503731 (cytochrome *b*, cyt*b*), and AY844266 (28S rRNA)) that maximised the number of mapped reads and mean coverage. We also attempted to map reads of hDNA to the nuclear genes proopiomelanocortin A (POMC), recombination activating-1 (RAG-1), rhodopsin exon 1 (RHOD), siah E3 ubiquitin protein ligase 1 (SIAH1), and tyrosinase (TYR), but coverage was inadequate. Finally, we called the consensus sequence using Geneious v. 11.0.5 (Kearse et al. 2012), based on the most commonly mapped nucleotide for each position and coverage depth greater than five.

## Phylogenetic analyses

Our character sampling included both phenomic and molecular data, following a total evidence approach (Kluge 1989). The phenomic dataset comprised the matrix of 201 characters scored by Orrico et al. (2021). The molecular data incorporated the newly generated hDNA sequences with Sanger sequencing data of three mitochondrial fragments (H1, *COI*, and cyt*b*) and five nuclear genes (POMC, RAG-1, RHOD, SIAH1, and TYR). GenBank accession numbers, voucher determinations, names in the tree, locality data, and references are available in Appendix S2.

Our taxon sampling included specimens of the *D. rubicundulus* clade as the ingroup. We selected multiple conspecific terminals to ensure geographic representation and enhance gene sampling per species. Our final ingroup sample included 63 terminals, with representatives of all eleven nominal species of the *D. rubicundulus* clade (including *D. araguaya* I and II; Orrico et al. 2021) and topotypic samples of *D. araguaya*, *D. cerradensis*, *D. jimi*, *D. rhea*, and *D. tritaeniatus*. We refer to vouchers potentially misidentified as *D. tritaeniatus* by Arantes et al. (2023) and not examined by Orrico et al. (2021) as *D.* cf. *tritaeniatus*. For outgroup delimitation, we employed successive outgroup expansion, a heuristic strategy in which new outgroup terminals are successively added until ingroup hypotheses remain stable for at least three rounds (Grant 2019). The first rounds sampled 6-10 representatives of the *D. branneri* clade (sister group of the *D. rubicundulus* clade); subsequent rounds added more distantly related representatives of Dendropsophini and Hylinae (Faivovich et al. 2005, Orrico et al. 2021). By doing so, we attempted to test ingroup relationships as severely as possible (Grant 2019). Terminals added in each round of expansion are listed in Appendix S2.

We conducted maximum parsimony (MP) analyses using direct optimisation in POY v. 5.1.1 (Wheeler et

al. 2015), in which nucleotide homology is tested by optimising unaligned DNA sequences directly onto alternative topologies (Wheeler 1996). We treated morphological characters statically. We employed the same partition breaks to maximise data inclusion as Orrico et al. (2021). We ran three 8 h searches on 704 CPUs (16,896 CPUh) with the command *search*, which implements random addition sequence Wagner builds (RAS; Farris 1970), subtree pruning and regrafting (SPR), tree bisection and reconnection (TBR) branch swapping (Goloboff 1996, 1999), ratcheting (Nixon 1999), and tree fusing (Goloboff 1999). For final refinement, we performed sectorial searches constrained by the strict consensus from the best trees from the previous searches (Goloboff 1999), followed by an exact iterative pass (Wheeler 2003a). We submitted the implied alignment (Wheeler 2003b) from the optimal tree to TNT v. 1.5 (Goloboff & Catalano 2016) using the command *xmult = level 10 chklevel 5 consense 5*. Finally, we computed Goodman-Bremer support (Goodman et al. 1982, Bremer 1988, Grant & Kluge 2008) using the bremer.run macro (available at http://www.lillo.org.ar/phylogeny/tnt); absolute frequencies of jackknife were calculated as resampling metric using the command *resample jak freq nogc replications 1000 [xmult = hits 5 level 2]* (Farris et al. 1996, Goloboff & Catalano 2016).

We performed maximum likelihood (ML) analysis using the outgroup sample from the last round of successive expansion in the MP analyses. We aligned sequences in MAFFT v. 7 (Katoh et al. 2019) using the algorithms E-INS-i for the H1 fragment and L-INS-i for other fragments (default costs for gap opening and extension). Next, we estimated the best-fitting models for each molecular partition using ModelFinder (Kalyaanamoorthy et al. 2017) implemented in IQ-TREE v. 2 (Minh et al. 2020). For morphology, we employed MK and ORDERED models for nonadditive and additive characters, respectively (see list of characters in Orrico et al. 2021), with ascertainment bias correction (Lewis 2001). To perform heuristic searches and compute the approximate likelihood ratio test (Guindon et al. 2010) and ultrafast bootstrap (1,000 pseudoreplicates), we used the command *iqtree2 -nt AUTO -cptime 300 -o Phyllodytes_luteolous_M -p CharacterSetsTE.txt -alrt 1000 -B 1000*. In addition, we used the MAFFT alignment with 16S rRNA (16Sar-L/16S) of the ingroup to calculate uncorrected pairwise distances within and between species in MEGA X (Kumar et al. 2018).

### Morphological analyses

All examined specimens are listed in Appendix S1. Collection abbreviations followed Sabaj (2020). We identified sex and maturity by inspection of gonads and secondary sexual characteristics (males with vocal slits on both sides were scored as adults; females with expanded oviducts and enlarged ova as adults). We studied the following characters under a Zeiss Discovery V8 stereomicroscope: dorsal colouration; number of sacral stripes on dorsum; number, contiguity, and orientation of anterior stripes on dorsum; eye protuberance; head shape; snout shape (Napoli & Caramaschi 1998, 1999a, b, 2000, Jansen et al. 2019). We studied the eight dorsal patterns defined by Napoli & Caramaschi (1999b): pattern A (two anterior and one sacral stripe discontinuous), B (many scattered dots), C (only the two anterior stripes), D (two anterior wave-like and one sacral stripe), E (only the sacral stripe), F (few scattered dots), G (immaculate), and H (straight, parallel, and well-marked stripes). We also studied an additional pattern (sacral stripe connected to the left and/or right anterior stripe; hereafter 'pattern I') reported by Bokermann (1965). Data from the following morphometric characters were taken from Napoli & Caramaschi (1998, 1999b): finger IV disk diameter (4FD), foot length (FL), head width (HW), interorbital distance (IOD), snout-vent length (SVL), thigh length (THL), tibia length (TL), and toe IV disk diameter (4TD). Finger numbering follows Fabrezi & Alberch (1996).

## Results

We successfully assembled hDNA from the paratopotypes of *D. rhea* and *D. tritaeniatus*. For *D. rhea*, we obtained 14,759,274 raw reads (GC = 50%; mean read length = 101 bp); after preprocessing, we recovered 6,925,905 reads (GC = 42%; mean read length = 34 bp); MITObim analyses successfully mapped a total of 4,216 reads to H1 (depth = 25.9×), *COI* (27.4×), and cyt*b* (27.0×). Likewise, we obtained 30,190,048 raw reads for *D. tritaeniatus* (GC = 49%; mean read length = 101 bp); after preprocessing, 12,718,604 reads remained (GC = 43%; mean read length = 36 bp); MITObim analyses mapped 14,631 reads to H1 (49.4×), *COI* (62.5×), cyt*b* (51.9×), and 28S (147.7×). Unfortunately, hDNA assembly was unsuccessful for the holotype of *D. araguaya*. See hDNA preprocessing results in Appendix S3 and a summary of assembly statistics in Table 1.

Our phylogenetic results revealed the position of *D. rhea* within a clade composed of *D. araguaya* I,

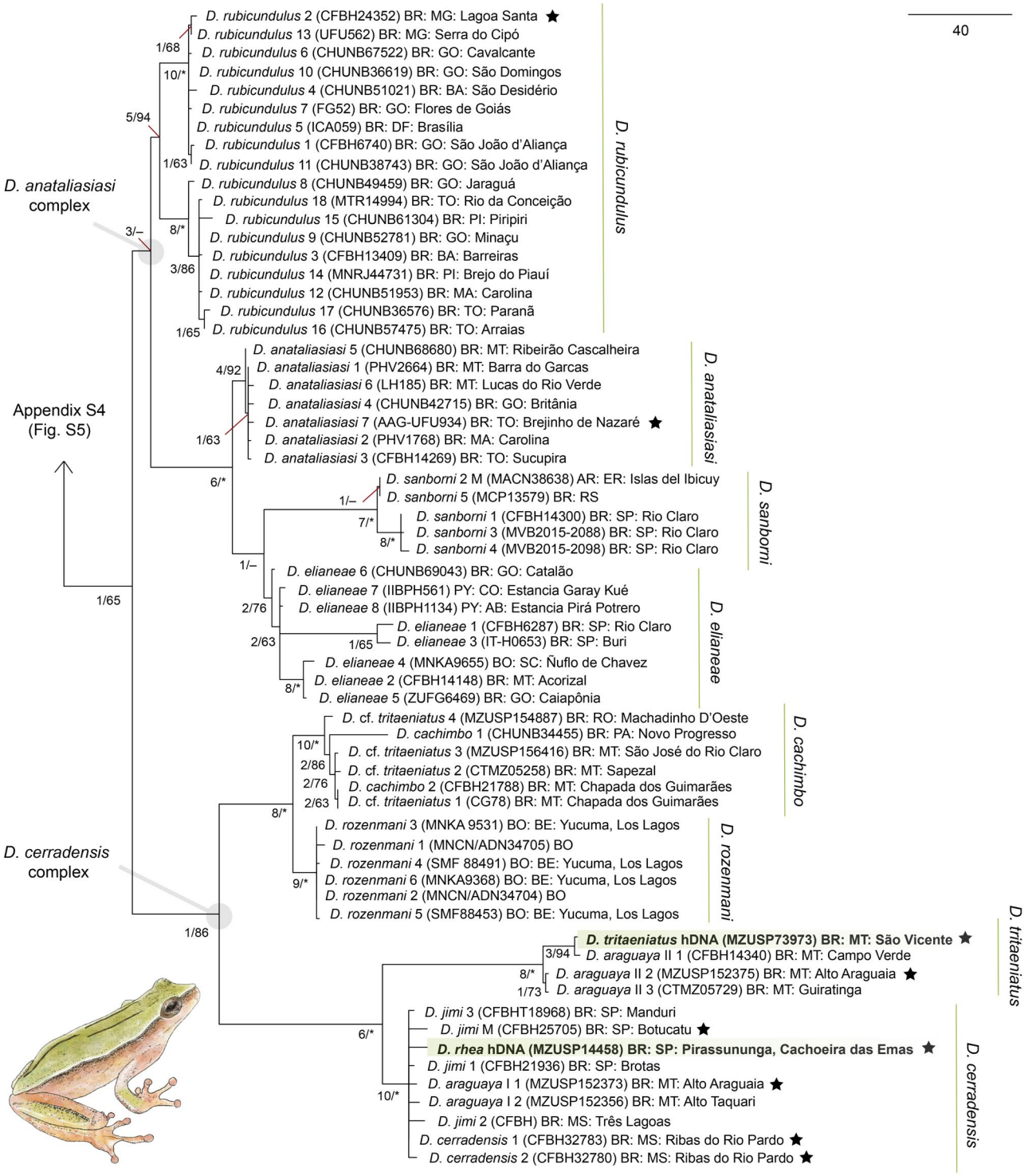


**Fig. 1.** Phylogenetic relationships of the *Dendropsophus rubicundulus* clade. Strict consensus tree recovered in the final round of outgroup expansion (13,653 steps). Numbers around nodes are Goodman-Bremer support/jackknife absolute frequencies. Asterisks indicate 100% jackknife values; < 50% values are omitted. Black stars indicate topotypic samples. Names next to green bars indicate the newly revised taxonomy. See the complete topology for MP and ML analyses in Appendix S4: Figs. S5 and S6, respectively. Abbreviations: AR – Argentina (provinces: ER – Entre Ríos); BO – Bolivia (departments: BE – Beni, SC – Santa Cruz); BR – Brazil (federative units: BA – Bahia, DF – Distrito Federal); GO – Goiás; MA – Maranhão; MS – Mato Grosso do Sul; MT – Mato Grosso; PA – Pará; PI – Piauí; RO – Rondônia; RS – Rio Grande do Sul; SP – São Paulo; TO – Tocantins); PY – Paraguay (departments: AB – Amambay, CO – Concepción).

*D. cerradensis*, and *D. jimi* (GB = 10, JK = 100%; Fig. 1). Furthermore, the paratopotype of *D. tritaeniatus* was placed among terminals of *D. araguaya* II (GB = 8, JK = 100%). The positions of *D. rhea* and *D. tritaeniatus* were consistent across all successive outgroup expansion rounds (Appendix S4: Figs. S1-S5) and optimality criteria (MP and ML trees; Appendix S4: Fig. S6 and Table S1). Uncorrected pairwise distances of 16S further revealed low genetic variation of 0-0.6% among *D. araguaya* I, *D. cerradensis*, *D. jimi*, and

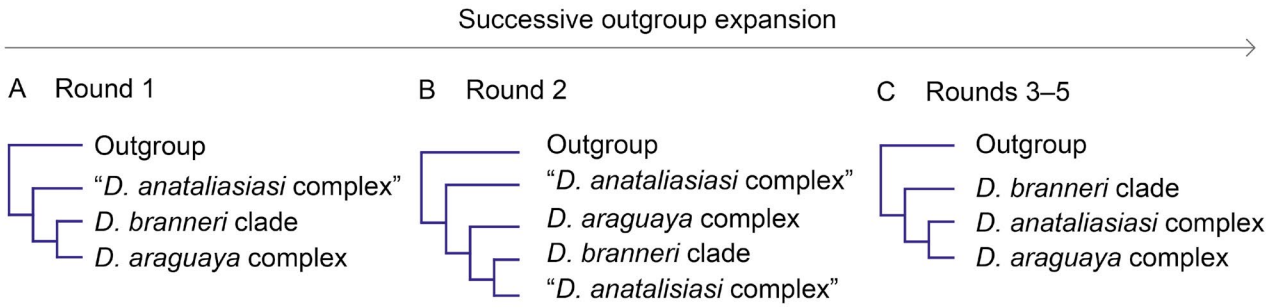


**Fig. 2.** Summary of changes in ingroup relationships throughout successive outgroup expansion. A) round 1; B) round 2; C) round 3-5. Outgroup taxa are omitted, except for the *Dendropsophus branneri* clade. See the complete topologies in Appendix S4.

**Table 1.** Summary of hDNA assembly results. See Appendix S3 for preprocessing results of all samples, including *D. araguaya*. Unambiguous consensus length refers to the number of nucleotides without IUPAC Ns.

| Species | Locus | Seed | # Mapped reads | Coverage depth | Unambiguous consensus length (bp) |
|---|---|---|---|---|---|
| *D. rhea* | H1 | MT503852 | 1,894 | 25.9 | 2,415 |
| | *COI* | MT483137 | 827 | 27.4 | 653 |
| | cyt*b* | MT503731 | 1,495 | 27.0 | 893 |
| *D. tritaeniatus* | H1 | MT503852 | 3,881 | 49.4 | 2,417 |
| | *COI* | MT483137 | 1,882 | 62.5 | 631 |
| | cyt*b* | MT503731 | 2,965 | 51.9 | 893 |
| | 28S | AY844266 | 5,903 | 147.7 | 604 |

*D. rhea*, low variation of 0-0.8% between *D. araguaya* II and *D. tritaeniatus*, and high variation of 4.3-5.3% between the two clades (Table 2, Appendix S5).

Relationships of some poorly supported groups varied throughout successive outgroup expansion (Fig. 2, Table 3). In round 1, the *D. rubicundulus* clade was paraphyletic due to the position of the *D. branneri* clade as a sister group of the *D. araguaya* complex (GB = 1, JK < 50%; Appendix S4: Fig. S1). Likewise, the *D. anataliasiasi* complex was also found paraphyletic due to the position of terminals of *D. rubicundulus*. In round 2, the *D. rubicundulus* clade and *D. anataliasiasi* complex remained paraphyletic, but the *D. branneri* clade changed its position, being poorly supported as a sister group of *D. rubicundulus* (GB = 2, JK < 50%; Appendix S4: Fig. S2). In all subsequent rounds with denser outgroup sampling (Appendix S4: Figs. S3-S5), the *D. branneri* clade was placed as a sister group of the *D. rubicundulus* clade, rendering the latter monophyletic, albeit with low support (GB = 1, JK = 53%). Likewise, the monophyly of the *D. anataliasiasi* complex is also supported, albeit weakly (GB = 3, JK < 50%), in rounds 3-5.

Morphometric analyses showed that previously proposed diagnostic characters overlap in *D. araguaya*, *D. cerradensis*, *D. jimi*, and *D. rhea* (Table 4). Likewise, morphological analyses revealed polymorphism in the dorsal colour patterns (Table 5).

## Discussion

### Museomics

The Darwinian shortfall has been problematic in *Dendropsophus* because 11 nominal species have not been included in phylogenetic analyses, including *D. amicorum* (Mijares-Urrutia, 1998), *D. battersbyi* (Rivero, 1961), *D. grandisonae* (Goin, 1966), *D. gryllatus* (Duellman, 1973), *D. limai* (Bokermann, 1962), *D. minimus* (Ahl, 1933), *D. pelidnus* (Duellman, 1989), *D. phlebodes* (Stejneger, 1906), *D. rhea*, *D. tintinabulum* (Melin, 1941), and *D. tritaeniatus*. Based on hDNA from formalin-fixed type material, we reduced the number of missing species from eleven to nine by determining the relationships of *D. rhea* and *D. tritaeniatus*. Although our samples were formalin-fixed 60-71 years prior to extraction, we obtained assemblies with a high mapping depth. In contrast, assemblies of the holotype of *D. araguaya* were unsuccessful, possibly due to a low amount of endogenous DNA. Future studies using target enrichment methods could increase the chance of

**Table 2.** Uncorrected *p* distances for partial 16S among species of the *Dendropsophus araguaya* complex. Minimum and maximum values are presented if n ≥ 3; otherwise, only a single pairwise distance can be calculated if n = 2, and it is not applicable if n = 1. The complete matrix of uncorrected *p* distances for each pair of samples in the *D. rubicundulus* clade is presented in Appendix S5.

| | | 1 | 2 | 3 | 4 | 5 | 6 | 7 | 8 | 9 |
|---|---|---|---|---|---|---|---|---|---|---|
| 1 | *D. araguaya* I (n = 2) | < 0.001% | | | | | | | | |
| 2 | *D. araguaya* II (n = 3) | 4.5-4.7% | 0.2-0.8% | | | | | | | |
| 3 | *D. cachimbo* (n = 2) | 7.9-8.0% | 7.1-7.9% | 0.8% | | | | | | |
| 4 | *D. cerradensis* (n = 2) | < 0.001% | 4.5-4.7% | 7.9-8.0% | < 0.001% | | | | | |
| 5 | *D. jimi* (n = 4) | 0-0.6% | 4.3-5.3% | 7.8-8.6% | 0.61-0.62% | 0-0.6% | | | | |
| 6 | *D. rhea* (n = 1) | < 0.001% | 4.5-4.7% | 7.9-8.0% | < 0.001% | 0-0.6% | NA | | | |
| 7 | *D. rozenmani* (n = 6) | 6.5-6.7% | 6.1-6.7% | 5.5-6.5% | 6.5-6.7% | 6.3-7.1% | 6.5-6.7% | 0-0.4% | | |
| 8 | D. cf. *tritaeniatus* (n = 4) | 7.9-8.0% | 6.3-8.0% | 0-2.0% | 7.9-8.0% | 7.8-8.6% | 7.9-8.0% | 5.5-6.5% | 0.4-2.1% | |
| 9 | *D. tritaeniatus* (n = 1) | 4.7-4.8% | 0-0.8% | 7.5-7.9% | 4.7-4.8% | 4.5-5.3% | 4.7% | 6.5-6.7% | 6.7-8.0% | NA |

successfully assembling the hDNA of this sample (e.g. Lyra et al. 2020).

## Ingroup relationships and outgroup expansion

Our ingroup relationships are overall congruent with previous hypotheses. For instance, within the *D. araguaya* complex, we corroborated the polyphyly of *D. araguaya* and *D. jimi*, as reported by Orrico et al. (2021). Furthermore, our results revealed that specimens of the former candidate species *D. cachimbo* A are nested within *D. elianeae* (Fig. 1, *D. elianeae* 4, 6, and 7; see also Jansen et al. 2011, 2019), corroborating the findings of Arantes et al. (2023).

Previous studies either corroborated (Orrico et al. 2021, Arantes et al. 2023, Portik et al. 2023) or refuted (Medeiros et al. 2013, Jansen et al. 2019) the monophyly of the *D. rubicundulus* clade, with Orrico et al. (2021) identifying one morphological synapomorphy (webbing insertion between toes I and II reaching subarticular tubercle I or the digital disc). However, some taxa related to the ingroup were unavailable for Medeiros et al. (2013) and Jansen et al. (2019), which could affect character optimisation and ingroup monophyly. Our results revealed that the monophyly of the *D. rubicundulus* clade is rejected in parsimony analyses employing small outgroup samples but is corroborated (albeit with low support) in analyses using denser outgroup samples. The same occurs with regard to the monophyly of the *D. anatalisiasi* complex in MP analyses. As such, we provided a new empirical example demonstrating the importance of outgroup sampling.

Unfortunately, careful delimitation of outgroup sampling is often neglected in systematics. On one hand, a large outgroup (e.g. sampling all species on GenBank) would be counterproductive because most computational effort would be directed at parts of the tree that are distant from the ingroup taxa related to the research question, which could both delay analyses unacceptably and prevent optimal ingroup topologies from being discovered during heuristic tree searches (Grant 2019). On the other hand, a small or inadequate (e.g. too distantly related to the ingroup) outgroup sample could affect ingroup relationships and character optimisation (e.g. Hillis 1998, Zwickl & Hillis 2002, Grant 2019). Our results corroborate previous studies showing the utility of successive outgroup expansion as a heuristic strategy for delimiting outgroup sampling, providing an empirical basis to strike a balance between a poorly delimited outgroup with few terminals and an unnecessarily large outgroup (Grant 2019, Anganoy-Criollo et al. 2022, Pires et al. 2023).

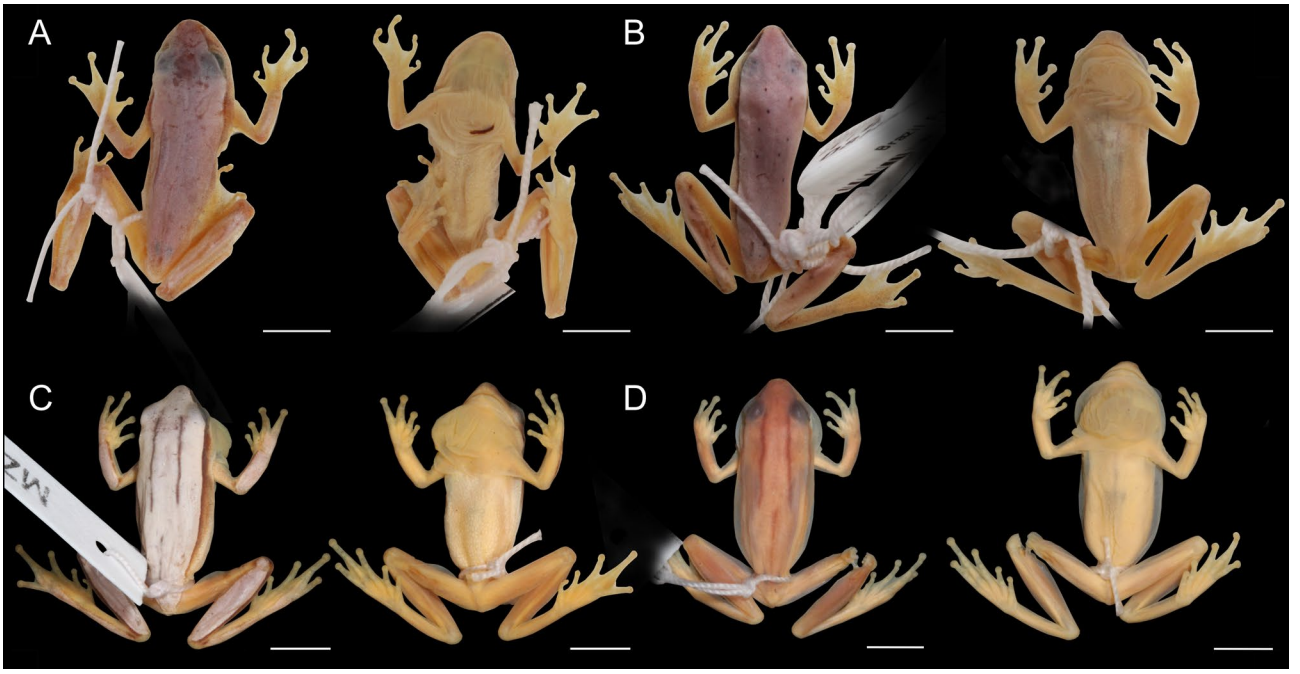


**Fig. 3.** Dorsal and ventral views of specimens of *Dendropsophus cachimbo* previously misidentified as *D. tritaeniatus*: A) MZUSP 156416; B) CFBH 21788. Note the immaculate dorsum, which differs from that of the type series of *D. tritaeniatus*, such as C) the paratopotype MZUSP 73973 and D) the holotype MZUSP 73656 (two parallel anterior stripes and one sacral stripe on dorsum). Scale bar – 5 mm.

## Taxonomy

The taxonomy of *Dendropsophus* suffers from Linnean shortfalls such as misidentifications and taxonomic inflation (e.g. Melo-Sampaio 2023, Arias-Cárdenas et al. 2024). Our study addresses some of these problems. Specifically, below we discuss four topics in the taxonomy of *D. araguaya* complex: 1) the misidentification of *D. tritaeniatus* specimens in previous studies, 2) the recognition of two synonyms of *D. cerradensis*, 3) the identity of *D. araguaya*, and 4) the appropriate name of the *D. araguaya* complex. We further discuss 5) distribution and 6) conservation.

### *Misidentification of* Dendropsophus tritaeniatus

Bokermann (1965) described *D. tritaeniatus* as a small treefrog from streams in São Vicente and Rondonópolis (Mato Grosso, Brazil) with three longitudinal dorsal stripes on a green background in life (violet in preservative). Recently, *D. cachimbo* and *D. rozenmani* were misidentified as *D. tritaeniatus* by Arantes et al. (2023) and Portik et al. (2023), respectively. Portik et al. (2023) misidentified MNKA 9531 (Los Lagos, Yucuma, Beni, Bolivia) as *D. tritaeniatus* (see their Fig. 41), thus overlooking that Bolivian populations previously determined as *D. tritaeniatus* are now assigned to *D. rozenmani* (Jansen et al. 2019). This error likely derives from MNKA 9531 being identified as *D. tritaeniatus* in GenBank (accession number JF790112), following the original identification in Jansen et al. (2011).

Some terminals referred to as *D. tritaeniatus* in Arantes et al. (2023) had previously been determined as *D. cachimbo*, including CFBH 21788 (Chapada dos Guimarães, Mato Grosso, Brazil), CHUNB 34455 (Novo Progresso, Pará, Brazil; Orrico et al. 2021), and UFU 1632 (Vilhena, Rondônia, Brazil; Jansen et al. 2019). However, Arantes et al. (2023) provided no justification for these re-identifications. They also reported new sequences from the tissues CTMZ 5258 (voucher unknown), 5675 (MZUSP 156416), and 16736 (MZUSP 154887) as *D. tritaeniatus*. Our examination of CFBH 21788 (*D. cachimbo* 2 in Fig. 1), MZUSP 156416 (*D.* cf. *tritaeniatus* 3), and 154887 (*D.* cf. *tritaeniatus* 4) revealed them to present an immaculate dorsum (as expected for *D. cachimbo*; Napoli & Caramaschi 1999a) instead of two anterior stripes and one sacral stripe (as expected for *D. tritaeniatus*; Fig. 3; Bokermann 1965). In addition, our phylogenetic results indicate that the paratopotype of *D. tritaeniatus* (MZUSP 73973) is distantly related to the aforementioned specimens. Likewise, genetic distances between hDNA of the paratopotype of *D. tritaeniatus* and samples of *D.* cf. *tritaeniatus* are 6.7-8.0% (well above the expected range for conspecifics in the *D. rubicundulus* clade), whereas those between *D. cachimbo* and *D.* cf. *tritaeniatus* are 0-2.0% (within the expected range for conspecifics; Table 2, Appendix S5). As such, the combined evidence from morphology, phylogeny, and genetic distances clarifies that these terminals identified as *D.* cf. *tritaeniatus* by Arantes et al. (2023) are actually *D. cachimbo*.

**Table 3.** Summary of results from outgroup sampling expansion. The position of *Dendropsophus rhea* and *D. tritaeniatus* are stable across all rounds. The monophyly of the *D. rubicundulus* clade was rejected in the first two rounds but was corroborated from rounds three to five. Tree costs from implied alignments analysed in TNT are omitted because no improvement was found. The same number of CPU hours were performed in all rounds. See the complete topologies in Appendix S4. Abbreviations: RAS – random addition sequences; DO – direct optimisation; IP – iterative pass; MPTs – most parsimonious trees.

| Round | # Outgroup terminals | Outgroup expansion summary | Root | Ingroup monophyly | # RAS | # Fuse | # Ratchets | DO cost | IP cost | # MPTs |
|---|---|---|---|---|---|---|---|---|---|---|
| 1 | 8 | +7 terminals of the *D. branneri* clade | *D. elegans* | Rejected | 113,847 | 3,171,813 | 57,145 | 3,281 | 3,279 | 260 |
| 2 | 25 | +17 terminals of *D. branneri* and *D. nanus* clades | *D. elegans* | Rejected | 116,957 | 2,240,085 | 58,617 | 5,455 | 5,443 | 63 |
| 3 | 33 | +8 terminals of the *D. microcephalus* group | *D. elegans* | Corroborated | 202,401 | 3,309,655 | 101,256 | 7,211 | 7,203 | 120 |
| 4 | 42 | +9 terminals of *Dendropsophus* | *P. luteolus* | Corroborated | 193,615 | 2,852,394 | 97,150 | 10,326 | 10,303 | 176 |
| 5 | 52 | +10 terminals of Hylinae | *P. luteolus* | Corroborated | 174,119 | 2,286,338 | 91,017 | 13,694 | 13,653 | 184 |

### *The identity of* **Dendropsophus cerradensis, D. jimi,** *and* **D. rhea**

Phylogeny, genetic distances, and morphology provide three sources of evidence that *D. cerradensis*, *D. jimi*, and *D. rhea* are conspecifics. First, our phylogenetic results placed *D. rhea* in a strongly supported clade with *D. araguaya* I, *D. cerradensis*, and *D. jimi* (GB = 10, JK = 100%; Fig. 1) that collapses in the strict consensus. Second, 16S distances among *D. cerradensis*, *D. jimi*, and *D. rhea* are 0-0.6% – below the ranges of interspecific variation found in the *D. rubicundulus* clade (Table 2). Third, although diagnostic characters were originally proposed (Napoli & Caramaschi 1998, 1999b), our morphological examinations indicate that they are intraspecifically variable and thus not diagnostic.

Napoli & Caramaschi (1998, 1999b) diagnosed *D. cerradensis*, *D. jimi*, and *D. rhea* from each other on the basis of the 1) orientation of the two anterior dorsal stripes (divergent in *D. cerradensis* and *D. rhea*; parallel in *D. jimi*), 2) contiguity of the two anterior dorsal stripes (discontinuous in *D. cerradensis* and *D. jimi*; both states in *D. rhea*), 3) protuberance of the eyes (less protuberant in *D. jimi*; more protuberant in *D. rhea*), 4) shape of the snout (truncate in *D. jimi*; pointed in *D. cerradensis*, and *D. rhea*), 5) 4FD (smaller in *D. rhea* than in *D. cerradensis*), 6) 4TD (smaller in *D. rhea* than in *D. cerradensis*), and 7) IOD (greater in *D. rhea* than in *D. cerradensis*). These characters, however, do not consistently diagnose *D. cerradensis*, *D. jimi*, and *D. rhea*. The patterns of anterior dorsal stripes are polymorphic among specimens (Fig. 4; see Table 2 in Napoli & Caramaschi 1999b), and eye protuberance and snout shape also overlap among them. For instance, some paratopotypes of *D. rhea* have less (e.g. MZUSP 30983; Fig. 4E) or more (e.g. MZUSP 30984) protuberant eyes (Fig. 4F). Likewise, some specimens of *D. jimi* do not have a truncate snout (e.g. MZUSP 134942 and 151019 in Figs. 4C, D). Among morphometric variables, ranges overlap in 4TD (0.7 mm in *D. cerradensis*; 0.4-0.7 mm in *D. rhea*) and marginally overlap in 4FD (0.5-0.7 mm in *D. rhea*, 0.7-0.8 mm in *D. cerradensis*) and IOD (1.7-2.1 mm in *D. cerradensis*, 2.1-2.6 mm in *D. rhea*).

Given our phylogenetic results, including topotypic samples, low genetic distances, and variation among putatively diagnostic characters, we consider *D. cerradensis*, *D. jimi*, and *D. rhea* to be conspecific. Although Arantes et al. (2023) did not propose taxonomic changes, our synonymisation is consistent with their finding that *D. cerradensis* and *D. jimi* could be conspecific according to species delimitation models

**Table 4.** Minimum and maximum values of morphometric variables previously reported as diagnostic for males of *Dendropsophus araguaya*, *D. cerradensis*, *D. jimi*, and *D. rhea*. All values are expressed in mm. Although not previously employed as diagnostic, SVL is also reported below. Abbreviations: FL – foot length; HW – head width; IOD – interorbital distance; SVL – snout-vent length; TL – tibia length; THL – thigh length; 4FD – finger IV disk diameter; 4TD – toe IV disk diameter.

| | *D. araguaya* | *D. cerradensis* | *D. jimi* | *D. rhea* |
|---|---|---|---|---|
| n | 16 | 6 | 42 | 42 |
| FL | 12.5-14.4 | 12.2-13.7 | 12.0-14.7 | 12.2-14.5 |
| HW | 5.8-6.3 | 5.8-6.2 | 5.2-6.3 | 5.5-6.5 |
| IOD | 2.0-2.5 | 1.7-2.1 | 1.8-2.5 | 2.1-2.6 |
| SVL | 18.9-20.5 | 18.9-19.3 | 17.6-20.9 | 17.6-20.7 |
| TL | 8.8-10.1 | 8.8-9.6 | 8.4-10.1 | 8.3-16.4 |
| THL | 8.8-9.9 | 8.6-9.2 | 8.5-10.1 | 8.2-10.2 |
| 4FD | 0.7-0.8 | 0.7-0.8 | 0.5-0.8 | 0.5-0.7 |
| 4TD | 0.6-0.8 | 0.7-0.7 | 0.5-0.8 | 0.4-0.7 |

**Table 5.** Variation in dorsal patterns of adult males of *D. araguaya*, *D. cerradensis*, *D. jimi*, *D. rhea*, and *D. tritaeniatus*. Pattern A – two anterior and one sacral stripe discontinuous; B – many scattered dots; C – only the two anterior stripes; D – two anterior wave-like and one sacral stripe; E – only the sacral stripe; F – few scattered dots; G – immaculate; H – three straight, parallel, and well-marked stripes; I – sacral stripe connected to the left and/or right anterior stripe.

| Species | n | A | B | C | D | E | F | G | H | I |
|---|---|---|---|---|---|---|---|---|---|---|
| *D. araguaya* | 26 | 5 | 0 | 2 | 11 | 1 | 3 | 4 | 0 | 0 |
| *D. cerradensis* | 5 | 0 | 0 | 0 | 4 | 0 | 1 | 0 | 0 | 0 |
| *D. jimi* | 44 | 12 | 12 | 2 | 0 | 2 | 10 | 6 | 0 | 0 |
| *D. rhea* | 43 | 0 | 0 | 4 | 34 | 0 | 2 | 3 | 0 | 0 |
| *D. tritaeniatus* | 43 | 9 | 0 | 1 | 3 | 0 | 0 | 0 | 28 | 2 |

using single nucleotide polymorphisms (missing for *D. rhea* in their study). Following the principle of priority (ICZN 1999: Art. 23.3), *D. jimi* (Napoli & Caramaschi 1999b) and *D. rhea* (Napoli & Caramaschi 1999b) are junior synonyms of *D. cerradensis* (Napoli & Caramaschi 1998). The ZooBank publication LSID is available at urn:lsid:zoobank.org:pub:E297E02C-351C-47CF-A9BB-8153C0EA87FC.

### *The identity of* **Dendropsophus araguaya**

Our results corroborate those of Orrico et al. (2021) concerning the polyphyly of *D. araguaya* (Fig. 1), with two independent lineages referred to as *D. araguaya* I (e.g. MZUSP 152356, 152373; Fig. 5A) and II (e.g. CFBH 14340 and MZUSP 152375; Fig. 5B), respectively. The 16S distance between these clades is 4.5-4.7%. Considering the position of these lineages, *D. araguaya* could be either a synonym of *D. cerradensis sensu novo* (with precedence to be determined; see comments below) or *D. tritaeniatus* (with *D. tritaeniatus* having precedence). However, the phylogenetic relationships of the holotype of *D. araguaya* must be determined to validate any taxonomic change, and our attempt to assemble hDNA of the holotype of *D. araguaya* failed. Furthermore, our morphological examinations of topotypes MZUSP 152373 (previously *D. araguaya* I, now *D. cerradensis sensu novo*; Fig. 5A) and MZUSP 152375 (previously *D. araguaya* II, now *D. tritaeniatus*; Fig. 5B) also failed to provide evidence to decisively associate the holotype of *D. araguaya* (Fig. 5C) with one of the lineages.

Napoli & Caramaschi (1998) diagnosed *D. araguaya* from *D. cerradensis* as being more robust (slender in *D. cerradensis*), having parallel anterior stripes on the dorsum (divergent in *D. cerradensis*), a rounded head (fusiform in *D. cerradensis*), and longer legs (shorter in *D. cerradensis*; operationally measured as FL, THL, and TL). Furthermore, *D. araguaya* was originally diagnosed from *D. tritaeniatus* as having a broader snout (narrow in *D. tritaeniatus*), rounded head (less rounded in *D. tritaeniatus*), and more intense colouration in preservative (less intense in *D. tritaeniatus*; Napoli & Caramaschi 1998). However, we found the morphological variation within *D. araguaya* to be much greater than expected, with all previously proposed characters being either poorly defined (e.g. colour 'intensity') or polymorphic and

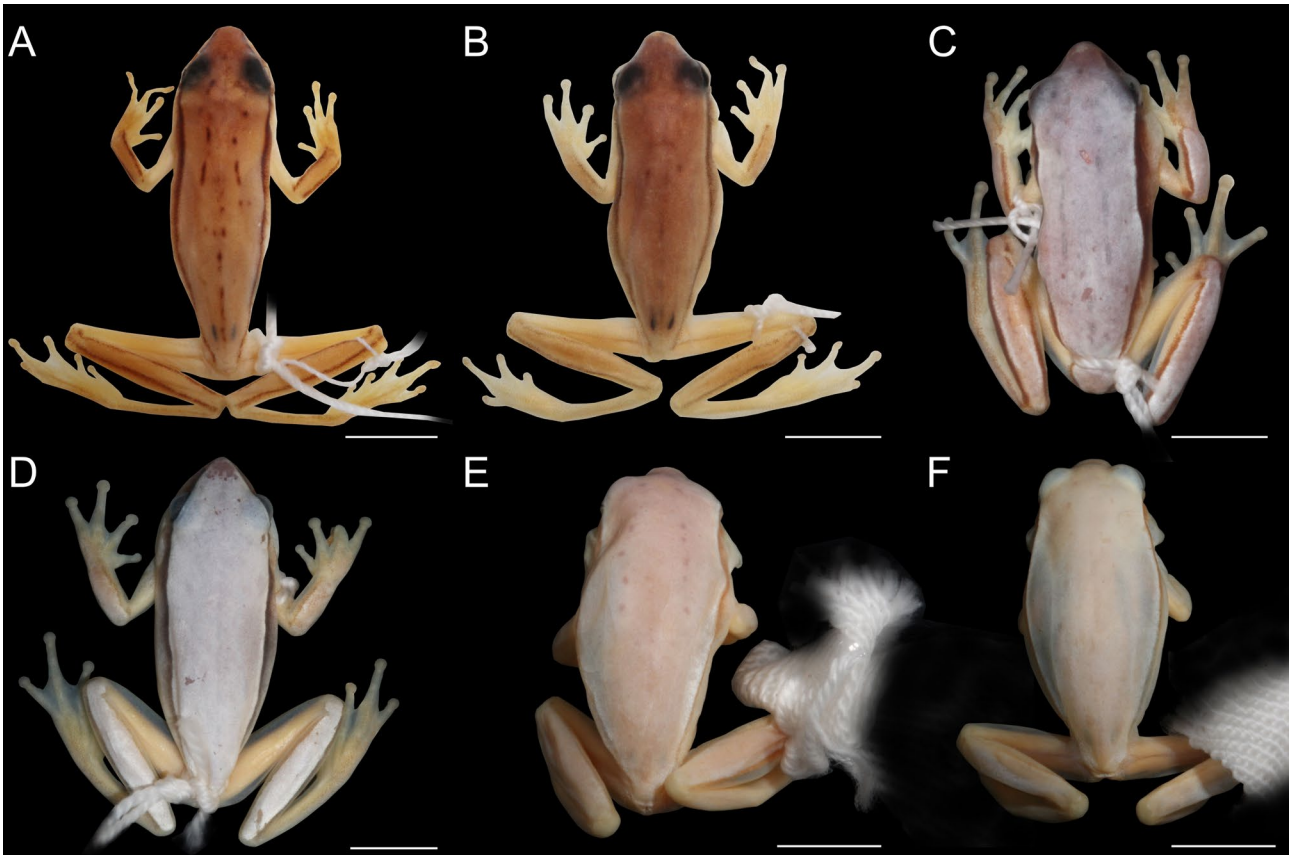


**Fig. 4.** Dorsal view of specimens of *Dendropsophus cerradensis* (senior synonym), *D. jimi*, and *D. rhea* (junior synonyms). *Dendropsophus cerradensis* in A) CFBH 32780 and B) CFBH 32781; *D. jimi*; C) MZUSP 134942; D) MZUSP 151019; *D. rhea*; E) MZUSP 30983; F) MZUSP 30984. Scale bar – 5 mm.

non-diagnostic (e.g. *D. araguaya* slender in topotypes MZUSP 152374 or robust in MZUSP 152377; head shape rounded in MZUSP 152375 or fusiform in MZUSP 152371; FL, THL, and TL overlap in *D. araguaya* and *D. cerradensis*; Table 4; anterior stripes absent in MZUSP 66806, parallel in MZUSP 66798, or divergent in MZUSP 152379; Table 5).

Therefore, we classify *D. araguaya* (Napoli & Caramaschi 1998) as *incertae sedis*. Furthermore, given the conflicting placement of topotypic specimens in different clades and the concomitant confusion surrounding the usage of the binomen, we invoke the Principle of First Reviser (ICZN 1999: Art. 24.2) to designate *D. cerradensis* (Napoli & Caramaschi 1998) as having precedence over *D. araguaya* (Napoli & Caramaschi 1998). Consequently, assuming the holotype is either *D. aragauaya* I or *D. araguaya* II, *D. araguaya* will be placed into the synonymy of either *D. cerradensis* or *D. tritaeniatus*, respectively.

### *The appropriate name for the* **Dendropsophus 'araguaya'** *complex*

Napoli & Caramaschi (1998, 1999b) defined the *D. tritaeniatus* complex with a specific composition: *D. araguaya*, *D. cerradensis*, *D. jimi*, *D. tritaeniatus*, and *D. rhea*. Subsequently, Jansen et al. (2019) noted that *D. rozenmani* was "morphologically most similar to the species in the *D. tritaeniatus* complex due to its striped dorsal pattern", but they did not change the composition of the group. Since Orrico et al. (2021) lacked sequences for *D. tritaeniatus*, and "to avoid confusion with previous groupings," they referred to the clade as the *D. araguaya* complex. However, given that available evidence strongly suggests that *D. araguaya* is a junior synonym of either *D. cerradensis* or *D. tritaeniatus*, it is problematic to continue referring to this clade as the *D. araguaya* complex. As such, we propose to name the clade composed of *D. cachimbo*, *D. cerradensis*, *D. rozenmani*, and *D. tritaeniatus* as the *D. cerradensis* complex.

### *The sympatry of* **Dendropsophus cerradensis** *and* **D. tritaeniatus**

*Dendropsophus cerradensis sensu novo* is broadly distributed throughout the Brazilian Cerrado in the federative units of Distrito Federal, Goiás, Mato Grosso, Mato Grosso do Sul, Minas Gerais, and São Paulo, as well as east-central Paraguay in the provinces of Amambay, Canindeyú, and San Pedro (Fig. 6; e.g. Weiler et al. 2013, Neves et al. 2019, Arantes et al. 2023). The sister group of *D. cerradensis* is *D. tritaeniatus*, whose populations occur northwest of *D. cerradensis* in the states of Mato Grosso and

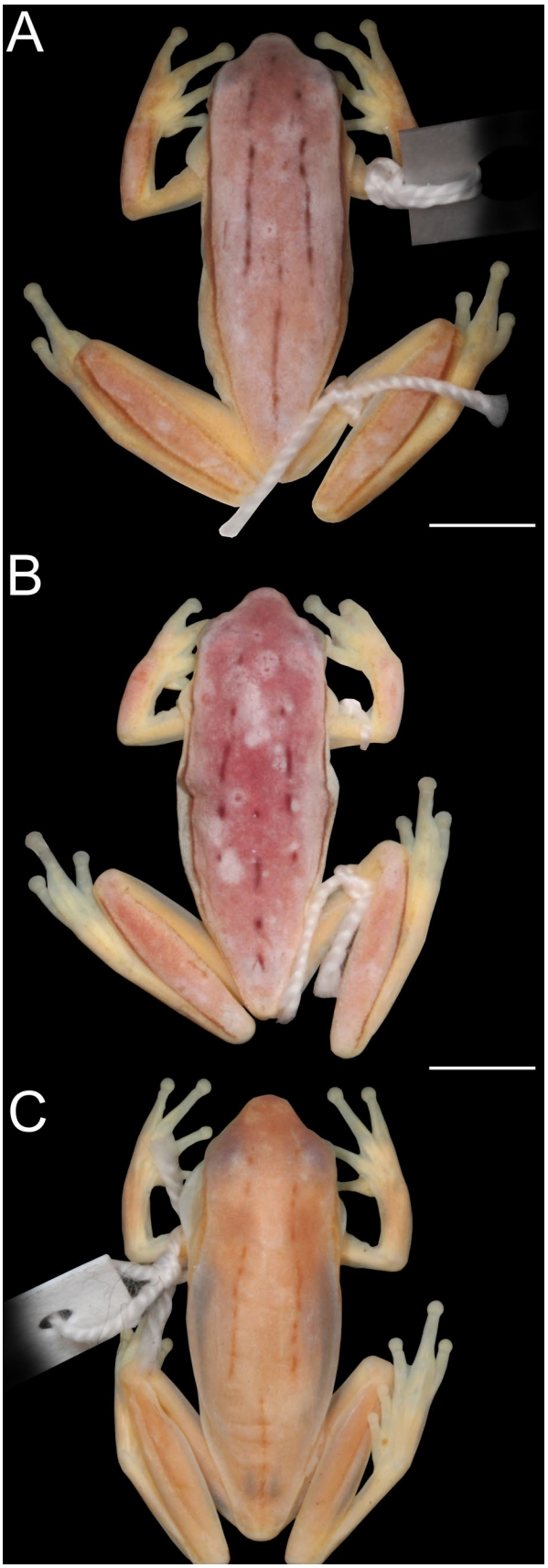


**Fig. 5.** Comparison of dorsal views of the two lineages of *Dendropsophus araguaya*. A) topotype MZUSP 152353 (referred to as *D. araguaya* I in Orrico et al. 2021, here corrected to *D. cerradensis*); B) topotype MZUSP 152375 (previously *D. araguaya* II, corrected to *D. tritaeniatus*); C) holotype MZUSP 66803 (*incertae sedis*). Scale bar – 5 mm.

Mato Grosso do Sul (Fig. 6; Bokermann 1965, Napoli & Caramaschi 1999a, Vaz-Silva et al. 2020). Notably, *D. cerradensis* and *D. tritaeniatus* co-occur in Alto do Araguaia, Mato Grosso, Brazil (i.e. type locality of *D. araguaya* incertae sedis), a contact zone between both species (Orrico et al. 2021).

Teixeira et al. (2013) and Teixeira & Giaretta (2015) reported that the advertisement calls of *D. cerradensis* and *D. tritaeniatus* are indistinguishable. However, the analysed calls of *D. cerradensis* were recorded at the type locality of the former *D. jimi* (Botucatu, São Paulo; Martins & Jim 2004) and Minas Gerais, whereas those of *D. tritaeniatus* were recorded in Chapada dos Guimarães, Mato Grosso (Teixeira et al. 2013). As such, the calls may only be indistinguishable in allopatry. Given the importance of advertisement calls as a premating isolation mechanism in anurans (Blair 1955, 1964, Bogert 1960) and the relatively high 16S distances between both species in sympatry (4.7%; Appendix S5), investigating calls from localities where both species co-occur is necessary to clarify how females distinguish between con- and heterospecific males. One possibility is reproductive character displacement, which results in heterospecific acoustic differentiation in sympatry (Fouquette 1960) and prevents the deleterious effects of hybridisation (i.e. reinforcement; Dobzhansky 1940) and signal interference (Howard 1993). Another possibility is that the advertisement calls of *D. cerradensis* and *D. tritaeniatus* are indistinguishable in sympatry due to allopatric speciation followed by a recent secondary contact (i.e. genetic drift could explain the accumulated differences in their mitochondrial DNA), in which case we would expect to either observe a high frequency of hybrids or some other premating isolation mechanism (e.g. temporal isolation or selection of different microhabitats). The available geographic and acoustic data is still limited, but it is notable that only one location has been identified where these species are sympatric (Orrico et al. 2021).

## Conservation

The current study illustrates that museomics can play a crucial role in resolving recalcitrant taxonomic problems, with important implications for conservation. Although many amphibians have been recently described from micro-endemic, threatened populations (e.g. Pie et al. 2013, Pinheiro et al. 2024), our revised taxonomy of *D. cerradensis* (senior synonym of *D. jimi* and *D. rhea*) expands its distribution. Given that many populations of *D. cerradensis sensu novo* occur in environmental protection areas (e.g. APA Corumbataí,

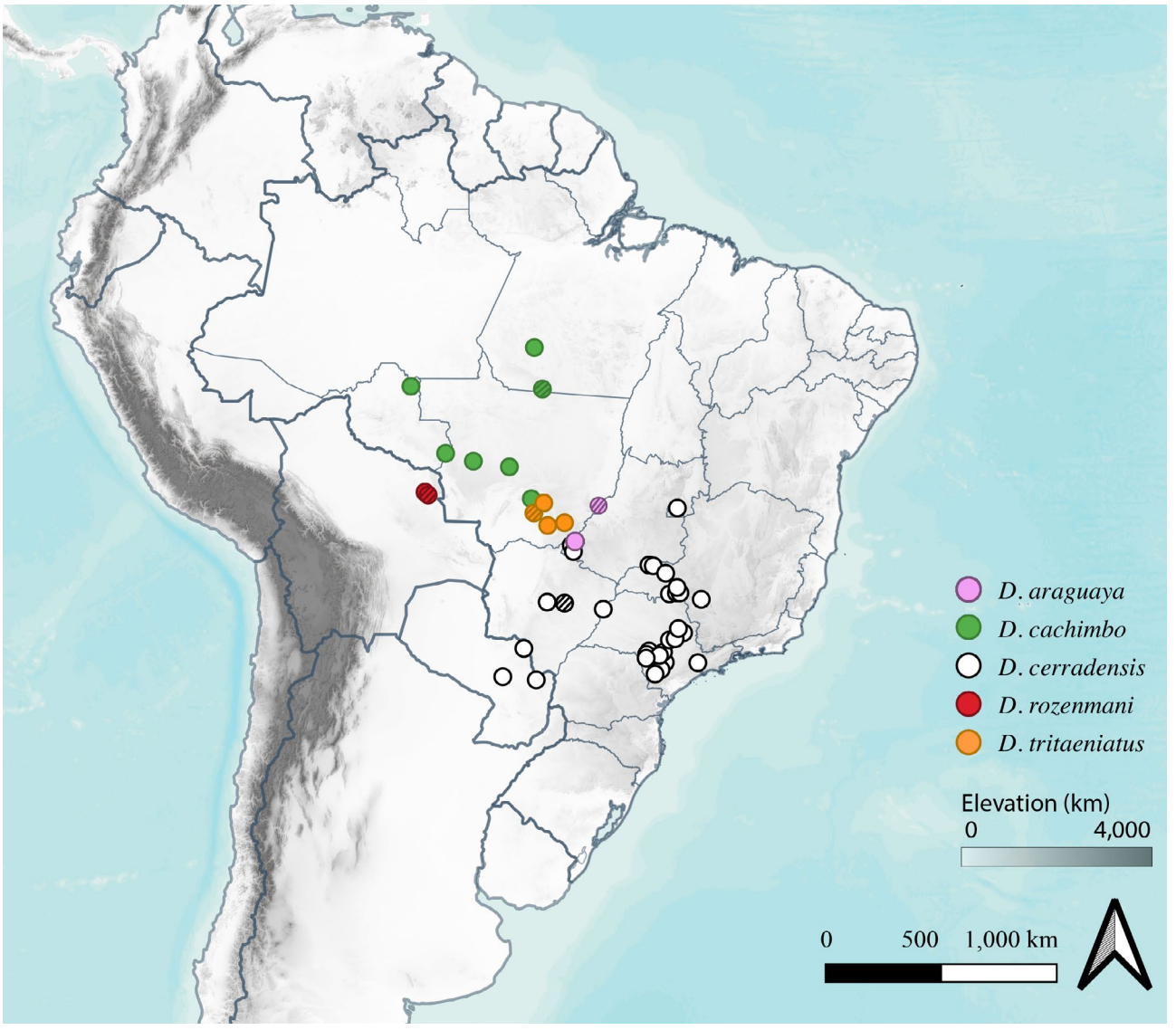


**Fig. 6.** Updated point distribution map of species of the *Dendropsophus cerradensis* complex, including *D. araguaya* incertae sedis, *D. cachimbo*, *D. cerradensis* (now senior synonym of *D. jimi* and *D. rhea*), *D. rozenmani*, and *D. tritaeniatus*. Circles with hatches indicate type localities.

Botucatu e Tejupá), state parks (e.g. Parque Estadual da Cantareira), national parks (e.g. Parque Nacional das Emas), and private natural heritage reserves (e.g. RPPN Olavo Egydio Setubal; IUCN 2024), its conservation status should be updated to 'Least Concern', following the classification of the former *D. jimi* (IUCN 2024). However, fieldwork is necessary to investigate whether topotypic populations of the former *D. rhea* at Cachoeira das Emas remain or have become locally extinct.

## Note added in proof

During the proofreading stage of this study, an additional contribution to the systematics of *Dendropsophus* was published. Whitcher et al. (2025) reconstructed the phylogeny of *Dendropsophus* using anchored hybrid enrichment (AHE) data, encompassing 432 nuclear loci for 78 species, combined with Sanger sequences and phenomic data (SP) from Orrico et al. (2021). The resulting phylogenomic matrix comprised 655,061 characters (more than 100 times larger than Orrico et al. 2021). To validate our conclusions, we performed a re-analysis incorporating our newly generated hDNA sequences of *D. rhea* and *D. tritaeniatus* with the AHE + SP data. Although differences are present in the internal relationships of the *D. anataliasiasi* complex, our hDNA + AHE + SP results revealed similar phylogenetic positions of *D. rhea* and *D. tritaeniatus* to those derived from hDNA + SP only (Appendix S4: Fig. S7). Specifically, we found *D. rhea* to be nested in a clade with *D. araguaya* I, *D. cerradensis*, and *D. jimi*, thereby validating our conclusion that *D. jimi* and *D. rhea* are junior synonyms of *D. cerradensis*.

## Acknowledgements

*C.F.B. Haddad, N. Pupin, D. Baêta, M. Vaini (CFBH), H. Zaher, and A.S. Benetti (MZUSP) allowed access to material under their care or provided relevant information on specimens. W. C. Wheeler provided equipment to D.Y.M. Nakamura at AMNH. C.S. Cassini provided valuable comments on the early versions of this manuscript. This research was funded by the Brazilian Fundação de Amparo à Pesquisa do Estado de São Paulo (FAPESP; grants #2012/12500-5 to V.G.D. Orrico, #2018/15425-0 to T. Grant, #2021/10639-5 to M.L. Lyra, #2022/02789-0 and #2024/03494-9 to D.Y.M. Nakamura) and Conselho Nacional de Desenvolvimento Científico e Tecnológico (CNPq #441614/2020-5, #310256/2020-8, and #312198/2023-0 to V.G.D. Orrico, #163546/2020-7 to M.L. Lyra, and 314480/2021-8 to T. Grant).*

## Author Contributions

*Conceptualisation: D.Y.M. Nakamura, T. Grant, and V.G.D. Orrico. Methodology: D.Y.M. Nakamura, M.L. Lyra, and T. Grant. Data collection: D.Y.M. Nakamura and E.M.G. da Silva. Data analyses: D.Y.M. Nakamura and E.M.G. da Silva. Writing (first draft): D.Y.M. Nakamura and V.G.D. Orrico. Writing (review and editing): all authors. Funding acquisition and supervision: T. Grant.*

## Data Availability Statement

*The newly generated hDNA sequences are available on GenBank:* D. rhea COI *(PQ763882), cyt*b *(PQ771667), and H1 (PVO23911);* D. tritaniatus COI *(PQ755211), cyt*b *(PQ771666), H1 (PVO23907), and 28S (PQ758633). Scripts, alignments, and trees are available at https://github.com/danimelsz/hDNA_Dendropsophus. This study was registered in ZooBank under the publication LSID urn:lsid:zoobank.org:pub:E297E02C-351C-47CF-A9BB-8153C0EA87FC.*

## Literature


Andrew S. 2010: FastQC, a quality control tool for high throughput sequence data. *http://www.bioinformatics.babraham.ac.uk/projects/fastqc*

Anganoy-Criollo M., Viuche-Lozano A., Enciso-Calle M.P. et al. 2022: The enigmatic *Hyloxalus edwardsi* species group (Anura: Dendrobatidae): phylogenetic position, a new species, and new putative morphological synapomorphies. *Herpetologica 78: 253–267*.

Arantes I.C., Vasconcellos M.M., Smith M.L. et al. 2023: Species limits and diversification of the *Dendropsophus rubicundulus* subgroup (Anura, Hylidae) in Neotropical savannas. *Mol. Phylogenet. Evol. 186: 107843*.

Arias-Cárdenas A., Barrientos L.S., Pardo-Diaz C. et al. 2024: Taxonomic inflation and a reconsideration of speciation in the Andes: the case of the high-elevation tree frog *Dendropsophus molitor* (Anura: Hylidae). *Zool. J. Linn. Soc. 200: 763–775*.

Blair W.F. 1955: Mating call and stage of speciation in the *Microhyla olivacea-M. carolinensis* complex. *Evolution 9: 469–480*.

Blair W.F. 1964: Isolating mechanisms and interspecies interactions in anuran amphibians. *Q. Rev. Biol. 39: 334–344*.

Blair M.E. 2024: Conservation museomics. *Conserv. Biol. 38: e14234*.

Bogert C.M. 1960: The influence of sound on the behavior of amphibians and reptiles. In: Lanyon W.E. & Tavolga W.N. (eds.), Animal sounds and communication. *American Institute of Biological Sciences, Washington, USA: 137–320*.

Bokermann W.C.A. 1965: Três novos batráquios da região central de Mato Grosso, Brasil. *Rev. Bras. Biol. 25: 257–264*.

Bremer K. 1988: The limits of amino acid sequence data in angiosperm phylogenetic reconstruction. *Evolution 42: 795–803*.

Dabney J., Knapp M., Glocke I. et al. 2013: Complete mitochondrial genome sequence of a Middle Pleistocene cave bear reconstructed from ultrashort DNA fragments. *Proc. Natl. Acad. Sci. U.S.A. 110: 15758–15763*.

Davis M.P., van Dongen S., Abreu-Goodger C. et al. 2013: Kraken: a set of tools for quality control and analysis of high-throughput sequence data. *Methods 63: 41–49*.

Diniz-Filho J.A.F., Loyola R.D., Raia P. et al. 2013: Darwinian shortfalls in biodiversity conservation. *Trends Ecol. Evol. 28: 689–695*.

Dobzhansky T. 1940: Speciation as a stage in evolutionary divergence. *Am. Nat. 74: 312–321*.

Duellman W.E. & Cole C.J. 1965: Studies of chromosomes of some anuran amphibians (Hylidae and Centrolenidae). *Syst. Zool. 14: 139–143*.

Duellman W.E. & Crump M.L. 1974: Speciation in frogs of the *Hyla parviceps* group in the upper Amazon basin. *Occas. Pap. Mus. Nat. Hist. 23: 1–40*.

Duellman W.E. & Trueb L. 1983: Frogs of the *Hyla columbiana* group: taxonomy and phylogenetic relationships. In: Rhodi A.G.J. & Miyata K. (eds.), Advances in herpetology and evolutionary biology. *Museum of Comparative Zoology, Harvard University, Cambridge, UK: 33–51*.

Ernst R., Kehlmaier C., Baptista N.L. et al. 2021: Filling the gaps: the mitogenomes of Afrotropical egg-guarding frogs based on historical type material and a re-assessment of the nomenclatural status of *Alexteroon* Perret, 1988 (Hyperoliidae). *Zool. Anz. 293: 215–224*.

Fabrezi M. & Alberch P. 1996: The carpal elements of anurans. *Herpetologica 52: 188–204*.

Faivovich J., Haddad C.F.B., Garcia P.C.A. et al. 2005: Systematic review of the frog family Hylidae, with special reference to Hylinae: phylogenetic analysis and taxonomic revision. *Bull. Am. Mus. Nat. Hist. 2005: 1–240*.

Farris J.S. 1970: Methods for computing Wagner trees. *Syst. Biol. 19: 83–92*.

Farris J.S., Albert V.A., Källersjö M. et al. 1996: Parsimony jackknifing outperforms neighbor-joining. *Cladistics 12: 99–124*.

Fouquette M.J. 1960: Isolating mechanisms in three sympatric treefrogs in the canal zone. *Evolution 14: 484–497*.

Frost D.R. 2024: Amphibian species of the world: an online reference, v.6.1. *Eletronic database, American Museum of Natural History, New York, USA. https://amphibiansoftheworld.amnh.org/index.php*

Fulton T.L. & Shapiro B. 2019: Setting up an ancient DNA laboratory. In: Shapiro B., Barlow A., Heintzman P. et al. (eds.), Ancient DNA: methods and protocols. *Humana Press, New York, USA: 1–13*.

Gansauge M.T., Gerber T., Glocke I. et al. 2017: Single-stranded DNA library preparation from highly degraded DNA using T4 DNA ligase. *Nucleic Acids Res. 45: e79*.

Goloboff P.A. 1996: Methods for faster parsimony analysis. *Cladistics 12: 199–220*.

Goloboff P.A. 1999: Analysing large data sets in reasonable times: solutions for composite optima. *Cladistics 15: 415–428*.

Goloboff P.A. & Catalano S.A. 2016: TNT version 1.5, including a full implementation of phylogenetic morphometrics. *Cladistics 32: 221–238*.

Goodman M., Olson C.B., Beeber J.E. & Czelusniak J. 1982: New perspectives in the molecular biological analysis of mammalian phylogeny. *Acta Zool. Fenn. 169: 19–35*.

Grant T. 2019: Outgroup sampling in phylogenetics: severity of test and successive outgroup expansion. *J. Zool. Syst. Evol. Res. 57: 748–763*.

Grant T. & Kluge A.G. 2008: Clade support measures and their adequacy. *Cladistics 24: 1051–1064*.

Guindon S., Dufayard J.F., Lefort V. et al. 2010: New algorithms and methods to estimate maximum-likelihood phylogenies: assessing the performance of PhyML 3.0. *Syst. Biol. 59: 307–321*.

Hahn C., Bachmann L. & Chevreux B. 2013: Reconstructing mitochondrial genomes directly from genomic next-generation sequencing reads – a baiting and iterative mapping approach. *Nucleic Acids Res. 41: e129*.

Hillis D.M. 1998: Taxonomic sampling, phylogenetic accuracy, and investigator bias. *Syst. Biol. 47: 3–8*.

Howard D.J. 1993: Reinforcement: origin, dynamics, and fate of an evolutionary hypothesis. In: Harrison R.G. (ed.), Hybrid zones and the evolutionary process. *Oxford University Press, Oxford, UK: 46–69*.

ICZN 1999: International Code of Zoological Nomenclature, 4th ed. *International Trust for Zoological Nomenclature, London, UK*.

IUCN 2024: The IUCN Red List of Threatened Species, v.2024-1. *https://www.iucnredlist.org*

Jansen M., Bloch R., Schulze A. & Pfenninger M. 2011: Integrative inventory of Bolivia's lowland anurans reveals hidden diversity. *Zool. Scr. 40: 567–583*.

Jansen M., Santana D.J., Teixeira B.F.V. & Köhler G. 2019: A new striped species of *Dendropsophus* (Anura: Hylidae) with a composite advertisement call and comments on the *D. rubicundulus* group. *Vertebr. Zool. 69: 227–246*.

Kalyaanamoorthy S., Minh B.Q., Wong T.K. et al. 2017: ModelFinder: fast model selection for accurate phylogenetic estimates. *Nat. Methods 14: 587–589*.

Katoh K., Rozewicki J. & Yamada K.D. 2019: MAFFT online service: multiple sequence alignment, interactive sequence choice and visualisation. *Brief. Bioinform. 20: 1160–1166*.

Kearse M., Moir R., Wilson A. et al. 2012: Geneious basic: an integrated and extendable desktop software platform for the organisation and analysis of sequence data. *Bioinformatics 28: 1647–1649*.

Kluge A.G. 1989: A concern for evidence and a phylogenetic hypothesis of relationships among *Epicrates* (Boidae, Serpentes). *Syst. Zool. 38: 7–25*.

Kumar S., Stecher G., Li M. et al. 2018: MEGA X: molecular evolutionary genetics analysis across computing platforms. *Mol. Biol. Evol. 35: 1547*.

Lewis P.O. 2001: A likelihood approach to estimating phylogeny from discrete morphological character data. *Syst. Biol. 50: 913–925*.

Llamas B., Valverde G., Fehren-Schmitz L. et al. 2017: From the field to the laboratory: controlling DNA contamination in human ancient DNA research in the high-throughput sequencing era. *Sci. Technol. Archaeol. Res. 3: 1–14*.

Lyra M.L., Lourenço A.C.C., Pinheiro P.D.P. et al. 2020: High-throughput DNA sequencing of museum specimens sheds light on the long-missing species of the *Bokermannohyla claresignata* group (Anura: Hylidae: Cophomantini). *Zool. J. Linn. Soc. 190: 1235–1255*.

Mahony S., Nidup T., Streicher J.W. et al. 2022: A review of torrent frogs (*Amolops*: Ranidae) from Bhutan, the description of a new species, and reassessment of the taxonomic validity of some *A. viridimaculatus* group species aided by archival DNA sequences of century-old type specimens. *Herpetol. J. 32: 142–175*.

Martin M. 2011: Cutadapt removes adapter sequences from high- throughput sequencing reads. *EMBnet J. 17: 10–12*.

Martin T.E., Bennett G.C., Fairbairn A. & Mooers A.O. 2022: 'Lost' taxa and their conservation implications. *Anim. Conserv. 26: 14–24*.

Martins I.A. & Jim J. 2004: Advertisement call of *Hyla jimi* and *Hyla elianeae* (Anura, Hylidae) in the Botucatu region, São Paulo, Brazil. *Braz. J. Biol. 64: 545–654*.

Medeiros L.R., Lourenço L.B., Rossa-Feres D.C. et al. 2013: Comparative cytogenetic analysis of some species of the *Dendropsophus microcephalus* group (Anura, Hylidae) in the light of phylogenetic inferences. *BMC Genet. 14: 1–18*.

Melo-Sampaio P.R. 2023: On the taxonomic status of *Dendropsophus koechlini* (Duellman & Trueb, 1989). *J. Vertebr. Biol. 71: 22023*.

Minh B.Q., Schmidt H.A., Chernomor O. et al. 2020: IQ-TREE 2: new models and efficient methods for phylogenetic inference in the genomic era. *Mol. Biol. Evol. 37: 1530–1534*.

Nakamura D.Y.M., Lyra M.L. & Grant T. 2024: Procedures for obtaining tissue samples from

amphibian and reptile specimens for museomics. *Herpetol. Bras. 13: 134–144*.

Napoli M.F. & Caramaschi U. 1998: Duas novas espécies de *Hyla* Laurenti, 1768 do Brasil central afins de *H. tritaeniata* Bokermann, 1965 (Amphibia, Anura, Hylidae). *Bol. Mus. Nac., N. S., Zool. 391: 1–12*.

Napoli M.F. & Caramaschi U. 1999a: Geographic variation of *Hyla rubicundula* and *Hyla anataliasiasi* with the description of a new species (Anura, Hylidae). *Alytes 16: 165–189*.

Napoli M.F. & Caramaschi U. 1999b: Variation and description of two new Brazilian *Hyla* of the *H. tritaeniata* complex (Amphibia, Anura, Hylidae). *Bol. Mus. Nac., N. S., Zool. 407: 1–11*.

Napoli M.F. & Caramaschi U. 2000: Description and variation of a new Brazilian species of the *Hyla rubicundula* group (Anura, Hylidae). *Alytes 17: 165–184*.

Neves M.O., Yves A., Pereira Silva E.A. et al. 2019: Herpetofauna in a highly endangered area: the Triângulo Mineiro region, in Minas Gerais State, Brazil. *Herpetozoa 32: 113–123*.

Nixon K.C. 1999: The parsimony ratchet, a new method for rapid parsimony analysis. *Cladistics 15: 407–414*.

Orrico V.G.D., Grant T., Faivovich J. et al. 2021: The phylogeny of Dendropsophini (Anura: Hylidae: Hylinae). *Cladistics 37: 73–105*.

Pie M.R., Meyer A.L.S., Firkowski C.R. et al. 2013: Understanding the mechanisms underlying the distribution of microendemic montane frogs (*Brachycephalus* spp., Terrarana: Brachycephalidae) in the Brazilian Atlantic Rainforest. *Ecol. Model. 250: 165–176*.

Pinheiro P.D.P., Dallacorte F., Thompson J. et al. 2024: Two new species of the *Boana semiguttata* clade (Anura: Hylidae: Hylinae) from the Atlantic Forest of Southern Brazil. *South Am. J. Herpetol. 33: 48–68*.

Pires C., Weksler M., Lanes R.O. et al. 2023: Systematics and biogeography of the Atlantic Forest endemic genus *Juliomys* (Rodentia: Cricetidae): a test of diversification hypothesis using mitochondrial data. *J. Mamm. Evol. 30: 695–712*.

Portik D.M., Streicher J.W. & Wiens J.J. 2023: Frog phylogeny: a time-calibrated, species-level tree based on hundreds of loci and 5,242 species. *Mol. Phylogenet. Evol. 188: 107907*.

Rancilhac L., Bruy T., Scherz M.D. et al. 2020: Target-enriched DNA sequencing from historical type material enables a partial revision of the Madagascar giant stream frogs (genus *Mantidactylus*). *J. Nat. Hist. 54: 87–118*.

Raxworthy C.J. & Smith B.T. 2021: Mining museums for historical DNA: advances and challenges in museomics. *Trends Ecol. Evol. 36: 1049–1060*.

Reyes-Velasco J., Goutte S., Freilich X. & Boissinot S. 2021: Mitogenomics of historical type specimens clarifies the taxonomy of Ethiopian *Ptychadena* Boulenger, 1917 (Anura, Ptychadenidae). *ZooKeys 1070: 135–149*.

Sabaj M.H. 2020: Codes for natural history collections in ichthyology and herpetology. *Copeia 108: 593–669*.

Shapiro B. 2017: Pathways to de-extinction: how close can we get to resurrection of an extinct species? *Funct. Ecol. 31: 996–1002*.

Straube N., Lyra M.L., Paijmans J.L. et al. 2021: Successful application of ancient DNA extraction and library construction protocols to museum wet collection specimens. *Mol. Ecol. Resour. 21: 2299–2315*.

Teixeira B.F.V. & Giaretta A.A. 2015: Setting a fundament for taxonomy: advertisement calls from the type localities of three species of the *Dendropsophus rubicundulus* group (Anura: Hylidae). *Salamandra 51: 137–146*.

Teixeira B.F.V., Giaretta A.A. & Pansonato A. 2013: The advertisement call of *Dendrospophus tritaeniatus*. *Zootaxa 3669: 189–192*.

Vaz-Silva W., Maciel N.M., Nomura F. et al. 2020: Guia de identificação das espécies de anfíbios (Anura e Gymnophiona) do Estado de Goiás e Distrito Federal, Brasil Central. *Sociedade Brasileira de Zoologia, Curitiba*.

Weiler A., Núñez K., Airaldi K. et al. 2013: Anfibios del Paraguay. San Lorenzo, Paraguay: Facultad de Ciencias Exactas y Naturales. *Universidad Nacional de Asunción – Universidad de Salamanca, San Lorenzo, Paraguay*.

Wheeler W.C. 1996: Optimisation alignment: the end of multiple sequence alignment in phylogenetics? *Cladistics 12: 1–9*.

Wheeler W.C. 2003a: Iterative pass optimisation of sequence data. *Cladistics 19: 254–260*.

Wheeler W.C. 2003b: Implied alignment: a synapomorphy-based multiple-sequence alignment method and its use in cladogram search. *Cladistics 19: 261–268*.

Wheeler W.C., Lucaroni N., Hong L. et al. 2015: POY version 5: phylogenetic analysis using dynamic homologies under multiple optimality criteria. *Cladistics 31: 189–196*.

Whitcher C., Orrico V.G.D., Ron S. et al. 2025: Phylogenetics, biogeography, and life history evolution in the broadly distributed treefrog genus *Dendropsophus* (Anura: Hylidae: Hylinae). *Mol. Phylogenet. Evol. 204: 108275*.

Whittaker R.J., Araújo M.B., Jepson P. et al. 2005: Conservation biogeography: assessment and prospect. *Divers. Distrib. 11: 3–23*.

Wingett S.W. & Andrews S. 2018: FastQ Screen: a tool for multi-genome mapping and quality control. *F1000Res. 7: 1338*.

Zwickl D.J. & Hillis D.M. 2002: Increased taxon sampling greatly reduces phylogenetic error. *Syst. Biol. 51: 588–598*.

## Supplementary online material

**Appendix S1.** List of examined specimens (https://www.ivb.cz/wp-content/uploads/JVB-vol.-74-2025-Nakamura-D.Y.M.-et-al.-Appendix-S1.pdf).

**Appendix S2.** GenBank accession numbers of sequences (https://www.ivb.cz/wp-content/uploads/JVB-vol.-74-2025-Nakamura-D.Y.M.-et-al.-Appendix-S2.xlsx).

**Appendix S3.** Additional historical DNA results (https://www.ivb.cz/wp-content/uploads/JVB-vol.-74-2025-Nakamura-D.Y.M.-et-al.-Appendix-S3.pdf).

**Appendix S4.** Additional phylogenetic results (https://www.ivb.cz/wp-content/uploads/JVB-vol.-74-2025-Nakamura-D.Y.M.-et-al.-Appendix-S4.pdf).

**Appendix S5.** Pairwise uncorrected *p* distances for 16S among all samples (https://www.ivb.cz/wp-content/uploads/JVB-vol.-74-2025-Nakamura-D.Y.M.-et-al.-Appendix-S5.xlsx).